

Neuropathological review of 138 cases genetically tested for X-linked hydrocephalus: evidence for closely related clinical entities of unknown molecular bases

Homa Adle-Biassette · Pascale Saugier-Weber · Catherine Fallet-Bianco · Anne-Lise Delezoide · Férecheté Razavi · Nathalie Drouot · Anne Bazin · Anne-Marie Beaufrère · Bettina Bessières · Sophie Blesson · Martine Bucourt · Dominique Carles · Louise Devisme · Frédérique Dijoud · Blandine Fabre · Carla Fernandez · Dominique Gaillard · Marie Gonzales · Frédérique Jossic · Madeleine Joubert · Nicole Laurent · Brigitte Leroy · Laurence Loeuillet · Philippe Loget · Pascale Marcorelles · Jelena Martinovic · Marie-José Perez · Daniel Satge · Martine Sinico · Mario Tosi · Jacques Benichou · Pierre Gressens · Thierry Frebourg · Annie Laquerrière

Received: 21 April 2013 / Revised: 15 June 2013 / Accepted: 17 June 2013 / Published online: 3 July 2013
© Springer-Verlag Berlin Heidelberg 2013

Abstract L1 syndrome results from mutations in the *LICAM* gene located at Xq28. It encompasses a wide spectrum of diseases, X-linked hydrocephalus being the most severe phenotype detected in utero, and whose pathophysiology is incompletely understood. The aim of this study was to report detailed neuropathological data from patients with mutations, to delineate the neuropathological criteria required for *LICAM* gene screening in fetuses by characterizing the sensitivity, specificity and positive predictive value of the cardinal signs, and

to discuss the main differential diagnoses in non-mutated fetuses in order to delineate closely related conditions without *LICAM* mutations. Neuropathological data from 138 cases referred to our genetic laboratory for screening of the *LICAM* gene were retrospectively reviewed. Fifty-seven cases had deleterious *LICAM* mutations. Of these, 100 % had hydrocephalus, 88 % adducted thumbs, 98 % pyramidal tract agenesis/hypoplasia, 90 % stenosis of the aqueduct of Sylvius and 68 % agenesis/hypoplasia of the corpus callosum. Two fetuses had *LICAM* mutations of unknown significance. Seventy-nine cases had no *LICAM* mutations; these were subdivided into four groups: (1)

H. Adle-Biassette and P. Saugier-Weber contributed equally to the work.

H. Adle-Biassette (✉)
Department of Pathology, Lariboisière Hospital, APHP,
2 Rue Ambroise Paré, 75010 Paris, France
e-mail: homa.adle@inserm.fr

H. Adle-Biassette · A.-L. Delezoide · P. Gressens
Inserm, U676, 75019 Paris, France

H. Adle-Biassette · A.-L. Delezoide · P. Gressens
UMRS 676, Univ Paris Diderot, Sorbonne Paris Cité,
75019 Paris, France

P. Saugier-Weber · N. Drouot · T. Frebourg
Department of Genetics, Rouen University Hospital,
Rouen, France

P. Saugier-Weber · M. Tosi · T. Frebourg
Inserm, U1079, Rouen, France

P. Saugier-Weber · M. Tosi · T. Frebourg · A. Laquerrière
Normandie University, IRIB, Rouen, France

C. Fallet-Bianco
Department of Pathology, Ste-Anne Hospital, APHP,
Paris, France

A.-L. Delezoide
Department of Biology of Development, Robert-Debré Hospital,
APHP, Paris, France

F. Razavi · B. Bessières
Department of Histology and Embryology, Necker Hospital,
APHP, Paris, France

A. Bazin
Department of Pathology and Cytogenetics, CERBA Laboratory,
Saint-Ouen l'Aumône, France

A.-M. Beaufrère
Department of Pathology, Clermont-Ferrand University Hospital,
Clermont-Ferrand, France

S. Blesson
Department of Medical Genetics and Foetopathology,
Tours University Hospital, Tours, France

M. Bucourt
Department of Pathology, Jean-Verdier Hospital,
APHP, Bondy, France

hydrocephalus sometimes associated with corpus callosum agenesis (44 %); (2) atresia/forking of the aqueduct of Sylvius/rhombencephalosynapsis spectrum (27 %); (3) syndromic hydrocephalus (9 %), and (4) phenocopies with no mutations in the *LICAM* gene (20 %) and in whom family history strongly suggested an autosomal recessive mode of transmission. These data underline the existence of closely related clinical entities whose molecular bases are currently unknown. The identification of the causative genes would greatly improve our knowledge of the defective pathways involved in these cerebral malformations.

Keywords X-linked hydrocephalus · Foetal neuropathology · *LICAM* genetic testing · Differential diagnosis · L1-like syndrome

Introduction

In 1949, Bickers and Adams [7] described a British family with several male sibs who died at birth from congenital hydrocephalus. Post-mortem examination revealed

structural brain abnormalities with narrowing of the aqueduct of Sylvius, which was assumed to be the cause of the hydrocephalus. The syndrome was named hydrocephalus due to stenosis of the aqueduct of Sylvius (HSAS). HSAS is the most common genetic form of congenital hydrocephalus, with a prevalence of approximately 1:30,000. It accounts for approximately 5–10 % of males with non-syndromic congenital hydrocephalus [12, 36].

HSAS belongs to a wide spectrum of phenotypes, now termed L1 syndrome, that range from severe to mild and that were thought to represent separate entities before the identification of the causative gene. The phenotypic spectrum of L1 syndrome, in addition to HSAS (OMIM#307000), includes MASA syndrome (mental retardation, aphasia, spastic paraplegia, adducted thumbs) (OMIM# 303350), SPG1 (X-linked complicated hereditary spastic paraplegia type 1) (OMIM#303350) and X-linked agenesis of the corpus callosum (OMIM#307000) [3, 6, 37, 47]. In fact, the severity of the disease can vary from severe hydrocephalus and prenatal death (HSAS subtype) to a milder phenotype (MASA syndrome subtype) or isolated agenesis of the corpus callosum, even within the same family [16, 37, 41].

D. Carles
Department of Pathology, Pellegrin University Hospital,
Bordeaux, France

L. Devisme
Department of Pathology, Lille University Hospital, Lille, France

F. Dijoud
Department of Pathology, Lyon University Hospital, Lyon,
France

B. Fabre
Department of Pathology, Grenoble University Hospital,
Grenoble, France

C. Fernandez
Department of Pathology, La Timone University Hospital,
Marseille, France

D. Gaillard
Department of Pathology and Cytogenetics, Reims University
Hospital, APHM, Reims, France

M. Gonzales
Foetopathology Unit, Trousseau Hospital, APHP, Paris, France

F. Jossic · M. Joubert
Department of Pathology, Nantes University Hospital, Nantes,
France

N. Laurent
Department of Pathology, Dijon University Hospital, Dijon,
France

B. Leroy · L. Loeuillet
Department of Pathology, Poissy Hospital, Poissy, France

P. Loget
Department of Pathology, Rennes University Hospital, Rennes,
France

P. Marcorelles
Department of Pathology, Brest University Hospital, Brest,
France

J. Martinovic
Department of Pathology, Antoine Beclère Hospital, APHP,
Clamart, France

M.-J. Perez
Department of Foetopathology and Medical Genetics,
Montpellier University Hospital, Montpellier, France

D. Satge
Department of Pathology, Tulle Hospital,
Tulle, France

M. Sinico
Department of Pathology, Créteil Hospital,
Créteil, France

J. Benichou
Department of Biostatistics and Methodology, Rouen University
Hospital, Rouen, France

A. Laquerrière
Department of Pathology, Rouen University Hospital, Rouen,
France

A. Laquerrière
NeoVasc Region-Inserm Team ERI28, Laboratory of
Microvascular Endothelium and Neonate Brain Lesions,
University of Rouen, Rouen, France

L1 syndrome is an X-linked recessive disease caused by mutations in the *LICAM* gene, located at Xq28, and consisting of 28 coding exons. In humans, the mature protein has 1,257 amino acids and is a transmembrane glycoprotein belonging to the immunoglobulin superfamily of cell adhesion molecules (CAMs). This glycoprotein contains, besides a signal peptide, 13 distinct domains including 6 immunoglobulin-like and 5 fibronectin III-like extracellular domains, one single-pass transmembrane domain and one short but highly conserved cytoplasmic domain. The L1 protein is known to mediate cell–cell adhesion at the cell surface. Using experimental studies, it has been demonstrated that L1 plays important roles in neuronal adhesion, neuronal migration, growth cone morphology [35], neurite outgrowth [46] and myelination [2]. The protein also plays an important part in the development of axonal tracts, path-finding and fasciculation, as well as in the development of the ventricular system and the cerebellum [5, 25]. In addition, L1 is involved in the regeneration of damaged nerve tissue [38] and has been implicated in long-term memory formation, synaptic plasticity and the establishment of long-term potentiation in the hippocampus [29, 44]. The non-neural expression of an alternatively spliced L1 lacking exons 2 and 27 has been described in intestinal crypt cells [40], in the male urogenital tract [24] and in leukocytes [23].

To date, >200 different *LICAM* mutations have been reported [43]. Most are unique to a single family, indicating that they are private mutations. Only a few families display the recurrence of a given mutation.

To our knowledge, only two previously published studies have reported a large series of patients suspected of L1 syndrome [12, 42]. In 2000, Finckh et al. [12] focused on phenotype–genotype correlations in a series of 153 patients suspected of harbouring *LICAM* mutations. Statistical analysis of the data indicated a significant effect on mutation detection rate of (1) family history; (2) the number of clinical findings typical of L1 disease; and (3) the presence or absence of signs not typically associated with L1 syndrome. In 2010, Vos et al. [42] studied 367 patients screened for *LICAM* mutations, and also looked for genotype–phenotype correlations. Both studies, however, used the same criteria for the inclusion of both prenatal and postnatal cases, even though some clinical parameters such as mental retardation or spastic paraplegia cannot be applied to foetal cases.

The aim of this work was to study a foetal population of 138 cases suspected of having L1 syndrome, and (1) to report detailed neuropathological data from mutated cases; (2) to delineate the neuropathological criteria required for *LICAM* gene screening in foetuses by characterizing the sensitivity, specificity and positive predictive value (PPV) of the six reported cardinal signs; and (3) to discuss the

differential diagnoses in non-mutant foetuses in order to delineate the neuropathological hallmarks of closely related conditions without *LICAM* mutations.

Materials and methods

Patients

A total of 138 DNA samples from 134 foetuses (14 weeks of gestation or WG to term) and 4 newborns (32, 36, 40 and 41 WG) who died at birth were referred from 32 French centres to the Department of Genetics of Rouen University Hospital from 1996 to 2011, for screening for *LICAM* mutations. Pregnancies were terminated with the informed consent of the parents and in accordance with the French law. Data regarding family history and foetal/antenatal clinical ultrasound (US) examinations were obtained in all cases. Foetopathological and neuropathological reports were available in all cases. These 138 cases were selected after the exclusion of cases with no neuropathological data, with macroscopic evidence for haemorrhagic-ischemic disease or evidence of in utero alcohol exposure (foetal alcohol syndrome).

Autopsy procedures and neuropathological examination

All cases underwent a complete autopsy performed by foetopathologists according to standardized protocols, including X-rays, photographs, and macroscopic and histological examination of all viscera. Foetal biometric data were assessed according to the morphometric criteria of Guihard-Costa et al. [19]. Autopsy reports, including neuropathological data, were carefully reviewed by two foetal neuropathologists (A.L., H.A.B.).

The presence or absence of the six major characteristics (cardinal signs) previously described was carefully verified [14, 26, 45]. In addition to male sex, they included adducted thumbs, hydrocephalus, corpus callosum abnormalities (complete or partial agenesis with or without Probst bundles, corpus callosum hypoplasia), stenosis of the aqueduct of Sylvius and abnormalities of the corticospinal tract. The latter consisted of hypoplasia/agenesis of the pyramids, alone or in combination with agenesis/hypoplasia of the corticospinal tracts in the mesencephalon and the pons, and lastly, in the spinal cord and in the internal capsule.

Brains were fixed in a 10 % buffered formalin solution. Brain growth was evaluated according to the biometric criteria of Guihard-Costa and Larroche [18]. Although brain weights and measurements were available for the majority of the foetuses, biometric data were taken into account cautiously due to the severity of the hydrocephalus, notably

in calculating the ratio between infratentorial versus total brain weight. It should be noted that in some cases, the severity of autolysis (4 cases) and of the hydrocephalus made it impossible to perform a complete neuropathological examination, in particular with regard to the analysis of the corpus callosum and of the septum (10 cases). In all cases, several tissue samples were embedded in paraffin. For histological analysis, 6- μ m sections were cut and stained with hematoxylin–eosin, and in some cases with cresyl violet.

L1CAM mutation screening

Blood samples were obtained after written informed consent for each patient and parents. Genomic DNA was extracted from blood samples using the Flexigene kit (Qiagen, Courtaboeuf, France). The 28 coding exons and intron–exon junctions of the *L1CAM* gene were PCR-amplified using 23 primer pairs (primer sequences and PCR conditions are available upon request). After purification, PCR products were sequenced with the same primers on an ABI Prism 3130 xl Genetic Analyser (Applied Biosystems) automated sequencer, using a BigDye Terminator v3.1 Cycle Sequencing Kit (Applied Biosystems, Courtaboeuf, France) according to the manufacturer's instructions. Nucleotide numbering for the mutations was done according to the reference cDNA sequence in GenBank Accession number NM_000425 (RefSeq NM_000425.3), in which the "A" of the start codon is nucleotide 1.

Statistical analyses

The sensitivity, specificity and positive predictive values of the various signs and Fisher's exact test were performed with Prism 5™ software.

Results

Genetic analyses

The sequencing of the entire coding region of the *L1CAM* gene identified deleterious mutations in 57 cases and variants of unknown significance (VUS) in 2 cases: c.400 + 27G>A in intron 4 and c.2209-6C>T in intron 17. These intronic variations are described neither in the Exome Variant Server (EVS), which groups data from the sequencing of 6500 exomes, nor in dbSNP135, which includes the data from the 1,000 Genome Project. However, since no splice change was predicted by five different bioinformatic tools (SpliceSiteFinder, MaxEntScan, NNSPLICE, GeneSplicer and Human Splicing Finder), the two VUS were excluded from subsequent studies.

The 57 male foetuses with deleterious mutations belonged to 54 distinct families: in 3 families, the mutations were recurrent, being present in 2 foetuses each. The presentation was familial for 24 foetuses and sporadic for 30 foetuses. In total, 49 distinct mutations were identified. Only two mutations were identified in more than one family: a nonsense mutation that was detected in two families (c.1453C>T; p.Arg485*) and a splice mutation detected in five families (c.400 + 5G>A; p.?). Thus, most of the mutations were private mutations. Missense mutations were detected in 16 patients (28.1 %), frameshift mutations (small deletions, duplications, insertions) in 13 patients (22.8 %), splice mutations in 14 patients (24.6 %), nonsense mutations in 12 patients (21.0 %) and large rearrangements in 2 patients (3.5 %). Detailed results are presented in Table 1.

Autopsy and neuropathological findings in foetuses and newborns with deleterious L1 mutations

Routine US examination performed at the beginning of the second trimester revealed hydrocephalus in all but two cases (Cases 25 and 56), in whom hydrocephalus was discovered during the third trimester. Hydrocephalus was either isolated or discovered in combination with corpus callosum agenesis (11 cases). Adducted thumbs were detected in 11 cases. A medical termination of the pregnancy was carried out in 52 cases (14–35 weeks WG) and 4 newborns died soon after birth (Cases 18, 19, 36 and 57). Only one foetus died in utero, at 24 weeks WG (Case 40).

General autopsy findings

At the time of autopsy, birth weight was normal in all but 2 cases, who displayed intrauterine growth retardation (Cases 15 and 45). No craniofacial dysmorphism was noted in any of the cases and only mild abnormalities were described related to hydrocephalus, consisting of macrocrania, hypertelorism, retrognathism and low-set ears. In two cases, a cleft palate was present (Cases 42 and 57). No skeletal abnormalities were found. Thymic hyperplasia and isolated unilateral renal agenesis were identified in Cases 15 and 28, respectively.

Neuropathological studies of foetuses with a disease-causing *L1CAM* mutation

Detailed macroscopic and microscopic findings are summarized in Tables 1 and 2. The percentage of foetuses and newborns displaying a specific sign was calculated by comparing the number of cases in whom the sign was present with the total number of cases in whom this criterion was evaluated. Cases where a change was "not evaluated" (not

Table 1 Cardinal signs in the 57 foetuses and newborns harbouring a *L1CAM* mutation

Case number	Position in the gene	Nucleotide change	Protein change	Nature of the mutation	Familial history	Age (WG)	Anomalies of upper and lower extremities	Hydrocephalus	Aqueductal stenosis	Corticospinal tract lesions	Corpus callosum anomalies	Number of positive cardinal signs
1	E01	c.-214_24del (c.-195_-156inv)	p.0?	Frameshift	S	29	BAT	1	S	PA, ASC	D	6
2	E03	c.118_119del	p.Gln40Val fs X12	Frameshift	S	24	UAT, C	1	0	ND	ND	3
3	E04	c.366del	p.Ala123ProfsX21	Frameshift	F	27	BAT	1	S	PA, CSH	ND	5
4	E09	c.1018del	p.Gln340ArgfsX50	Frameshift	F	27	BAT	1	S	PA, ICH	CCA	6
5	E10	c.1227del	p.His410ThrfsX20	Frameshift	F	20	BAT	1	ND	PA	CCA	5
6	E10	c.1211_1212ins11	p.Cys404X	Frameshift	F	21	BAT	1	S	PA	D	6
7	E15	c.1917del	p.Asp640ThrfsX53	Frameshift	F	28	0	1	S	PA	ND	4
8	E16	c.1986_1995dup	p.Gly666ValfsX26	Frameshift	S	24	BAT, DA	1	S	PA	D	6
9	E21	c.2796dup	p.,Ser933GlnfsX28	Frameshift	F	24	UAT	1	S	PH, ICA	ND	5
10	E22	c.2933_2934del	p.His978GlnfsX25	Frameshift	F	21	BAT	1	S	PA, CSH	CCA	6
11	E23	c.3114del ^a	p.Lys1039ArgfsX64	Frameshift	F	24	BAT, C	1	S	PA	CCA	6
12	E24	c.3197del	p.Gln1066ArgfsX37	Frameshift	S	28	BAT, C	1	S	PA, CSA	CCA	5
13	E25	c.3453_3456del	p.Tyr1151X	Frameshift	S	25	ND	1	S	PA, CSH	D	5
14	E01-E28	Triplex gene	p.?	Large rearrangement	F	29	ND	1	S	CSH	N	4
15	E03-E28	c.92-?_*1147 + ?del	p.?	Large rearrangement	S	31	BAT	1	S	PA, CSH	CCA	6
16	E04	c.208A>C	p.Thr70Pro	Missense	F	34	BAT	1	S	PA, ICH	PCA	6
17	E07	c.803G>A	p.Gly268Asp	Missense	S	32	BAT	1	S	PA, CSH	CCA	6
18	E08	c.935G>A	p.Cys312Tyr	Missense	F	32 PD	ND	1	S	PA, ICH	CCA	5
19	E10	c.1156C>T	p.Arg386Cys	Missense	F	36 PD	ND	1	0	ND	ND	2
20	E10	c.1211G>A	p.Cys404Tyr	Missense	S	24	BAT	1	S	PA	CCA	6
21	E12	c.1417C>T	p.Arg473Cys	Missense	F	25	0, C	1	S	PH	PCA	5
22	E12	c.1380G>C ^b	p.Trp460Cys	Missense	S	26	BAT, DA	1	S	PA	ND	5
23	E13	c.1630G>A	p.Asp544Asn	Missense	F	27	0	1	0	PA, CSH	CCA	4
24	E13	c.1630G>A	p.Asp544Asn	Missense	F	29	UAT	1	S	PH, CSH	ND	5
25	E14	c.1765T>C	p.Tyr589His	Missense	F	35	BAT	1	S	ND	ND	4
26	E14	c.1765T>C	p.Tyr589His	Missense	F	14	BAT	ND	ND	ND	ND	Not relevant at this age
27	E16	c.2120T>G	p.Val707Gly	Missense	S	35	BAT	1	S	PH	D	6
28	E18	c.2254G>A	p.Val752Met	Missense	F	23	BAT	1	S	PA, CSH	PCA	6
29	E18	c.2384G>T ^c	p.Gly795Val	Missense	S	24	BAT, DA	1	S	PA, CSH	PCA	6
30	E23	c.3074C>A	p.Ala1025Asp	Missense	F	24	0, C	1	ND	ND	D	3
31	E24	c.3239T>C	p.Leu1080Pro	Missense	S	25	BAT, C	1	S	PA	CCA	6
32	E06	c.621C>A ^d	p.Tyr207X	Nonsense	S	24	UAT	1	S	PH, CSH	D	6

Table 1 continued

Case number	Position in the gene	Nucleotide change	Protein change	Nature of the mutation	Familial history	Age (WG)	Anomalies of upper and lower extremities	Hydrocephalus	Aqueductal stenosis	Corticospinal tract lesions	Corpus callosum anomalies	Number of positive cardinal signs
33	E07	c.772C>T	p.Gln258X	Nonsense	S	25	0	I	S	PA, ICH, CSA	CCA	5
34	E08	c.871C>T	p.Gln291X	Nonsense	F	24	BAT, DA	I	S	PA, CSH	D	6
35	E08	c.892C>T	p.Gln298X	Nonsense	S	29	BAT	I	ND	ND	ND	3
36	E12	c.1380G>A	p.Trp460X	Nonsense	S	40 PD	BAT	I	S	PH	CCA	6
37	E12	c.1453C>T	p.Arg485X	Nonsense	S	22	BAT	I	S	ND	D	5
38	E12	c.1453C>T	p.Arg485X	Nonsense	S	24	BAT	I	ND	PA	CCA	5
39	E15	c.1882C>T	p.Gln628X	Nonsense	F	24	BAT	I	S	PH, CSH	CCA	6
40	E16	c.1989C>G	p.Tyr663X	Nonsense	S	24 IUD	BAT, C	I	S	PA, CSA	D	6
41	E21	c.2785C>T	p.Gln929X	Nonsense	S	26	BAT	I	ND	CSH	CCA	5
42	E23	c.3163G>T	p.Gly1055X	Nonsense	S	23	BAT, HE I	I	S	PA, CSA, ASC	PCA	6
43	E23	c.3107G>A ^e	p.Trp1036X	Nonsense	F	25	BAT	I	ND	ND	ND	3
44	I01	c.76 + 5G>A	p.?	Splice	S	33	BAT	I	0	PH, CSH	ND	4
45	I04	c.400 + 5G>A	p.?	Splice	F	24	BAT, DA	I	S	PA	CCA	6
46	I04	c.400 + 5G>A	p.?	Splice	F, T1	24	BAT	I	S	PH, CSH	D	6
47	I04	c.400 + 5G>A	p.?	Splice	F, T2	24	BAT	I	S	PH, CSH	ND	5
48	I04	c.400 + 5G>A	p.?	Splice	S	28	BAT	I	ND	PA, CSH	CCA	5
49	I04	c.400 + 5G>A	p.?	Splice	S	26	BAT	I	S	ISH, PH	CCA	6
50	I04	c.400 + 5G>A	p.?	Splice	S	30	BAT	I	S	PH, CSH	CCA	6
51	I05	c.523 + 12C>T	p.?	Splice	S	23	BAT	I	S	PH, CSH	D	6
52	I07	c.807-6G>A	p.?	Splice	F	23	BAT	I	0	0	CCA	4
53	I10	c.1267 + 1G>A	p.?	Splice	F	22	BAT, DA	I	S	CSH	D	6
54	I13	c.1704-75G>T	p.?	Splice	S	24	0	I	S	PH, CSH	CCA	5
55	I15	c.1940-1G>A	p.?	Splice	S	26	BAT	I	S	PA, CSH	CCA	6
56	I21	c.2872 + 1G>A	p.?	Splice	S	35	BAT	I	S	ND	CCA	5
57	I24	c.3323-2A>G ^f	p.?	Splice	S	41 PD	BAT	I	S	PA, CSA, ASC	D	6

Total signs: number of positive cardinal signs (a non-determined cardinal sign was considered negative)

0 normal, ASC agenesis of the corticospinal tract in the spinal cord, BAT bilateral adducted thumbs, C camptodactyly, CCA complete corpus callosum agenesis, CSA corticospinal tract agenesis, CSH corticospinal hypoplasia, D dysmorphic corpus callosum, DA distal arthrogyria, E exon, F familial, HE I hyperextension of the first toe, I intron, ICA agenesis of the internal capsule, IUD intrauterine death, ND not determined, PA pyramidal agenesis, PCA partial corpus callosum agenesis, PD perinatal death, PH pyramidal hypoplasia, S stenosis, Sp sporadic, T1 and T2 twin number one and two, UAT unilateral adducted thumbs, WG weeks of gestation

^a Presence of an additional nucleotide variation of unknown significance: c.2107G>T (p.Val703Phe)

^b Presence of two additional nucleotide variations of unknown significance: c.3323-84C>T (p.?) and c.3458-34C>T (p.?)

^c Presence of two additional nucleotide variations of unknown significance: c.992-32C>T (p.?) and c.2302G>A (p.Val768Ile)

^d Presence of an additional nucleotide variation of unknown significance: c.618C>A (p.Asp206Glu)

^e Presence of an additional nucleotide variation of unknown significance: c.3178G>A (p.Gly1060Arg)

^f Presence of two additional nucleotide variations of unknown significance: c.984C>T (p.Thr328Thr) and c.2848G>C (p.Gly950Arg)

Table 2 Summary of cardinal signs in 135 fetuses and newborns with and without any mutation in *LICAM* gene, their sensitivity and specificity for the diagnosis of *LICAM* gene mutation

Groups	Number of cases	Males	Hydrocephalus ^a	Adducted thumbs ^a	Corpus callosum abnormalities ^a	Stenosis of the aqueduct of Sylvius ^a	Corticospinal tract abnormalities ^a	% fetuses with 5 or more criteria ^b
X-linked hydrocephalus	56	100 % (56/56)	100 % (56/56)	88.5 % (46/52)	97.7 % (43/44)	89.8 % (44/49)	97.9 % (47/48)	80.4 % (45/56)
Aqueductal atresia spectrum	21	85.7 % (18/21)	100 % (21/21)	16.7 % (3/18)	66.7 % (10/15)	0 % (0/19)	64.3 % (9/14)	4.8 % (1/21)
Polymalformative syndromes	7	85.7 % (6/7)	85.7 % (6/7)	50 % (1/2)	60 % (3/5)	66.7 % (4/6)	0 % (0/3)	0 (0/7)
CNS malformations	35	85.7 % (30/35)	71.4 % (28/35)	15.4 % (4/26)	77.4 % (24/31)	45 % (9/20)	47.6 % (10/21)	2.9 % (1/35)
LICAM-like	16	87.5 % (14/16)	100 % (16/16)	61.5 % (8/13)	75 % (12/16)	93.7 % (15/16)	87.5 % (14/16)	75 % (12/16)
Sensitivity (%)			100	88.46	97.73	89.80	97.92	
Specificity (%)			10.13	71.93	26.87	64.70	62.07	

^a For statistical analyses of cardinal signs, cases where a sign was not determined were excluded. The incidence of a cardinal sign among the population was calculated by the ratio of the number of cases with positive cardinal signs to the number of cases in whom the cardinal sign was determined

^b Ratio of the number of cases with 5 or 6 positive cardinal signs (a non-determined cardinal sign was considered as negative) to the total number of cases

mentioned in the report, or not reported even if present) and Case 26 at 14 WG, an age at which the corpus callosum begins to develop, were excluded from calculations of the sensitivity, specificity and positive predictive value of the signs.

Generally the neuropathological phenotype of the 57 cases was homogeneous, and in almost all cases, the brain surface was smooth, with a reduction or absence of sulci and gyri. Hydrocephalus was present in all reported cases (Fig. 1c) except for Case 26 at 14WG, and was triventricular in 49 cases and biventricular in 7 cases (Fig. 1d). An associated dilatation of the fourth ventricle was noted in Case 19.

Adducted thumbs were present in 46/52 cases (88.5 %) (Fig. 1a), bilaterally in 43 cases and unilaterally in 4. In 35 cases, no other anomalies of the extremities were detected; in these adducted thumbs were bilateral in 32 cases and unilateral in 3. Among the other cases, bilateral adducted thumbs were described in combination with camptodactyly in four cases (Fig. 1b), with distal arthrogryposis of the four limbs in six cases, and with hyperextension of the big toe in one case. Unilateral adducted thumb with camptodactyly was noted in one case. Two cases displayed camptodactyly not associated with adducted thumbs.

Stenosis of the aqueduct of Sylvius, which is characterized by the narrowing of the lumen and the absence of

circular ependyma-lined channels, was identified in 89.8 % (44/49) of the cases (Figs. 1e, 2a and a normal aqueduct in a mutated case Fig. 2b), in combination with stenosis of the fourth ventricle in one case (Case 4) and of the third ventricle in nine cases (Cases 1, 2, 4, 17, 18, 29, 39, 42 and 57). A single case had tetraventricular dilatation (Case 19).

Corpus callosum examination was impossible in 12 cases due to prolonged post-mortem delay and severity of the hydrocephalus. In addition, it could not be performed in Case 26, at 14 GW, since at this stage the development of the corpus callosum, which reaches its mature form at 20 weeks, is incomplete. Various abnormalities were reported in 43/44 cases (97.7 %). Complete agenesis was identified in 24 cases, with Probst bundles (Figs. 1f, 2d, e) described in a single neuropathological report, and partial agenesis was identified in 5. Other abnormalities considered as “dysmorphic”, such as a flattened, hypoplastic, stretched or thin corpus callosum, were observed in 14 cases. The corpus callosum was normal in one case.

Corticospinal tracts were abnormal in 47/48 (97.9 %) cases. Pyramidal agenesis was observed in 28 cases (58 %) (Figs. 1g, 2f). Internal capsule hypoplasia, agenesis and/or fragmentation were observed in four cases (Cases 4, 9, 16 and 18) (Fig. 2g). Although spinal cord examination was carried out in eight cases only, pyramidal tracts were absent in three of these (37.5 %).

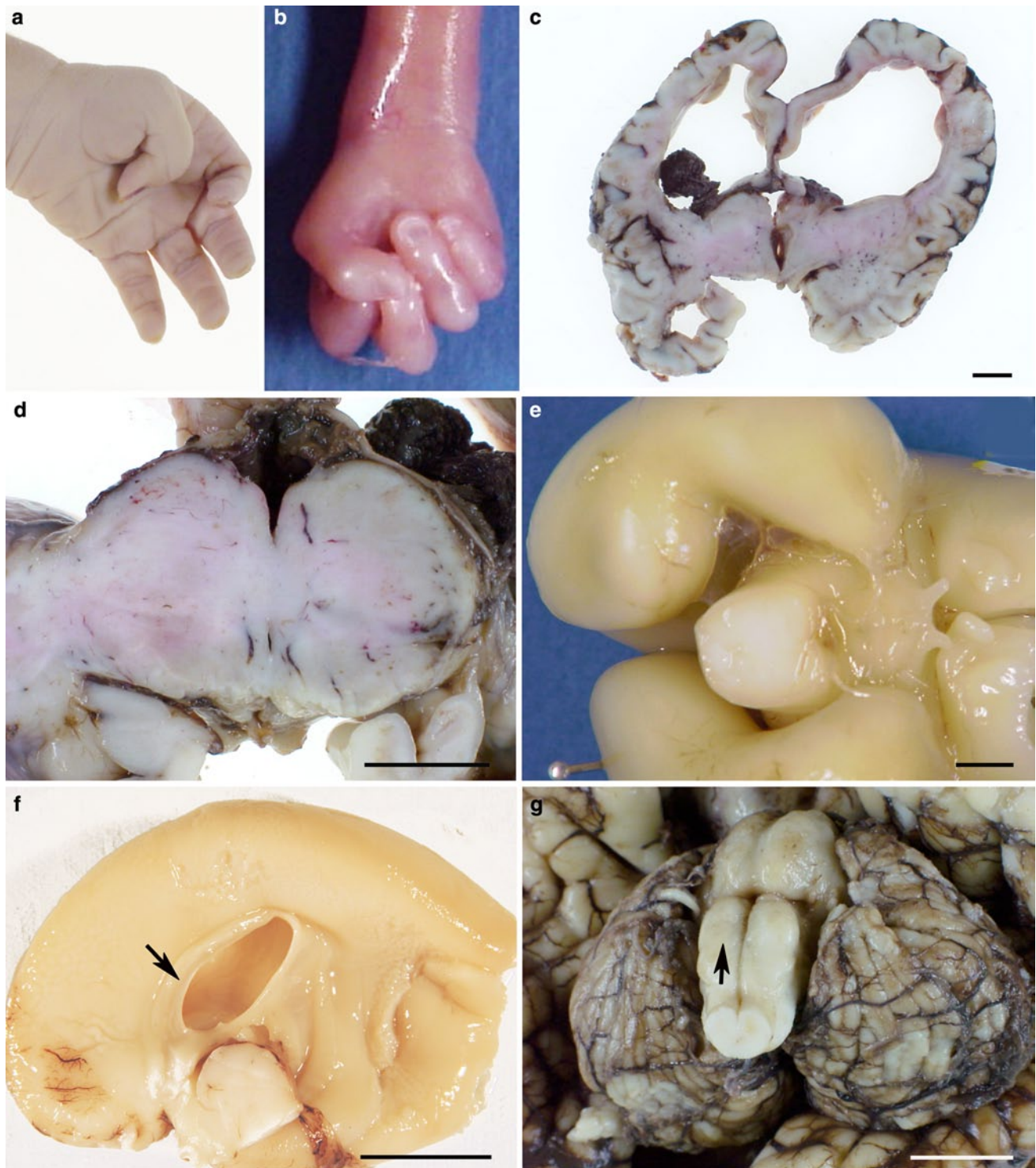


Fig. 1 Macroscopic patterns of antenatal and neonatal L1 syndrome: **a** adducted thumbs in a mutated newborn (case 57). **b** Adducted thumbs with bilateral camptodactyly (case 11). **c** Coronal section passing through the diencephalon revealing severe hydrocephalus and agenesis of the corpus callosum, with no associated anomalies (case 57). **d** Apparently fused thalami due to severe collapse of the third ventricle (case 57). **e** Coronal section passing through the cerebral

peduncles, with no patent aqueduct of Sylvius, (case 11). **f** Median sagittal section of the cerebral hemispheres displaying agenesis of the corpus callosum with the presence of Probst bundles (*arrow*) (case 11). **g** Antero-inferior view of the brainstem and cerebellum. Absence of pyramidal tracts, contrasting with prominent inferior olivary nuclei (*arrow*) (case 57) (*scale bar* 1 cm)

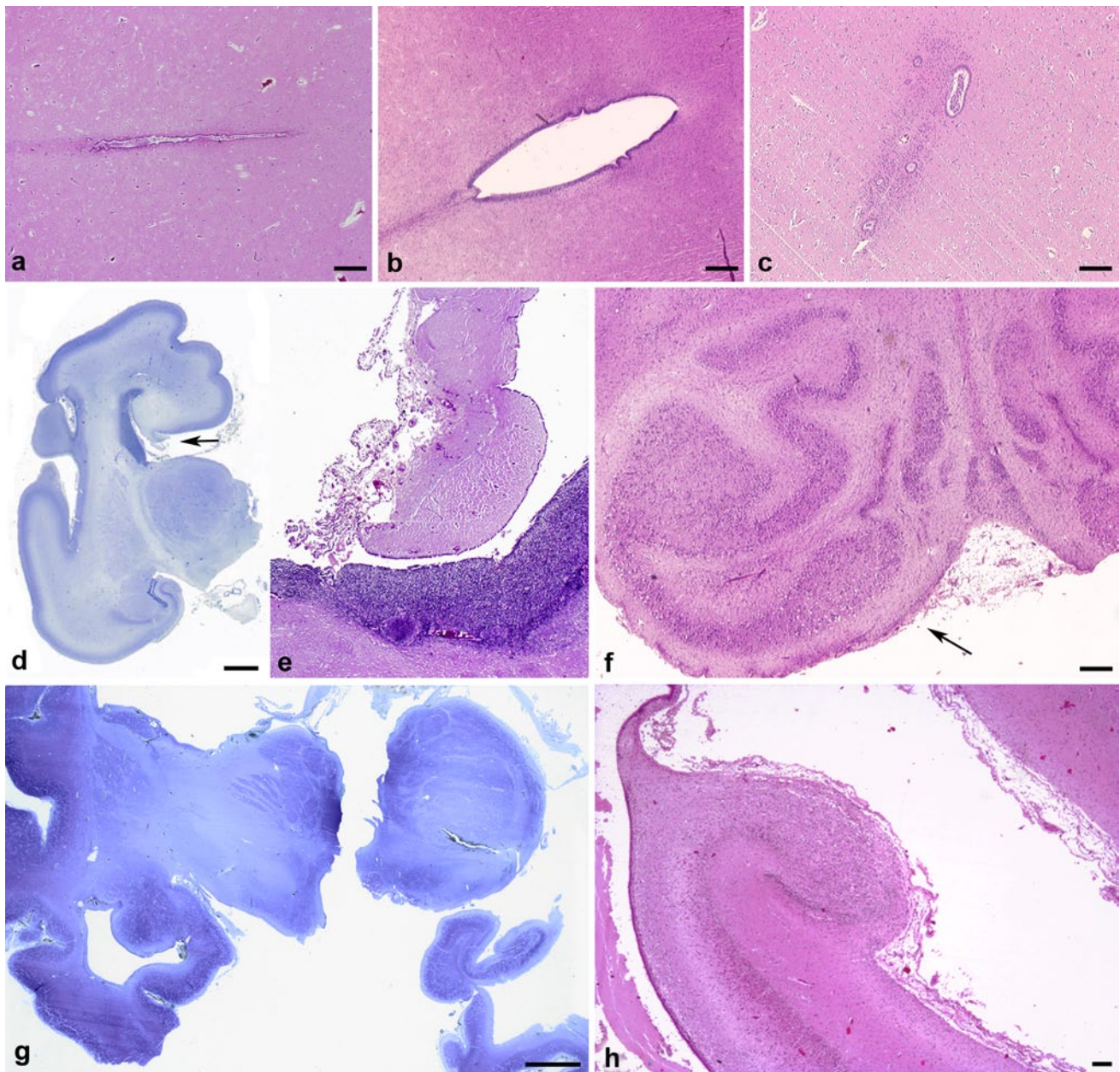


Fig. 2 Main histological findings in L1 syndrome: **a** isolated stenosis of the aqueduct of Sylvius, with neither deformation of the lumen nor atresia-forking of the aqueduct (case 11) [OM $\times 100$]. **b** For comparison, normal aqueduct of Sylvius in a mutated case at 22 GW [OM $\times 100$]. **c** And atresia-forking of the aqueduct of Sylvius, consisting of rudimentary disseminated ependymal channels [OM $\times 100$]. **d** Histological pattern of Probst bundles at low magnification (*arrow*) in a case of corpus callosum agenesis without mutation in *LICAM* **e** With

callosal axons arranged in whorls instead of running across the midline (same case) [OM $\times 25$]. **f** Agenesis of the pyramids, with olivary nuclei spreading out on the anterior side of the medulla along the arcuate nucleus (*arrow*) [OM $\times 100$]. **g** Microscopic view of internal capsule abnormalities: fragmentation and distortion of axonal bundles (case 57). **h** Severely hypoplastic dentate gyrus (Case 9) OM: original magnification, (*scale bar a, b, c, f* 50 μm , **h** 100 μm and **d, g** 1 cm)

At the infratentorial level, mild or moderate abnormalities could be observed in some cases. Brainstem and cerebellar weights as well as transverse diameter measurements were available in 36 cases. Infratentorial biometric data were normal in 25 cases. In six cases, biometric data were inferior to the 5th percentile (Cases 21, 26, 29, 36, 47

and 49) while in five cases, they were superior to the 95th (Cases 16, 35, 40, 54 and 52).

Histologically, cortical lamination was normal. No heterotopic neurons were observed in the intermediate zone. Olfactory bulb agenesis was observed in only one case (Case 49). The thalami and basal ganglia were normal in

40 cases. They were abnormally shaped in 11 cases (Cases 4, 17, 18, 28, 29, 39, 44, 46, 49, 52 and 54), hypoplastic in 4 cases (Cases 16, 33, 40 and 49) and fragmented in 1 case (Case 16). In seven cases, they appeared to be apposed or fused due to the collapse of the third ventricle (Cases 1, 2, 17, 18, 23, 39 and 57). The ependymal lining was normal, although in some cases, abrasion foci secondary to hyperpression in the ventricular system were observed. Migrational abnormalities were never observed. The hippocampi were sometimes distorted and displaced but no cytoarchitectural abnormality was observed, except in one case in which the dentate gyrus was hypoplastic and incomplete (Fig. 2h). The brainstem nuclei were normal. Incidental findings consisting in micropolygyria were observed in two cases likely secondary to the excessive folding of the cortical plate (Cases 6 and 9, Fig. 3a). In another case, the brain surface was pachygyric (Case 57, Fig. 3b). In the medulla, the inferior olivary nucleus was heterotopic in a single case (Case 9, Fig. 3c). A tectal hamartoma was identified in a single case (Case 11, Fig. 3d). Hypoplasia of the vermis was identified in Case 30 only, and dysplastic or fragmented dentate nuclei were observed in 6 cases (Cases 9, 20, 21, 23, 32 and 56, Fig. 3e).

Neuropathological characteristics of fetuses and newborns without a disease-causing L1 mutation

Seventy-nine fetuses and newborns did not display any mutation in the *LICAM* gene. The neuropathological review allowed us to classify patients into four distinct subgroups (Table 2).

Twenty-one fetuses, of which 85.7 % were males, belonged to the aqueductal atresia spectrum, which includes atresia-forking of the aqueduct of Sylvius (Fig. 2c) consisting of absent permeable lumen, replaced by several small tubules lined by ependymal cells. This abnormality is sometimes associated with rhombencephalosynapsis, fusion of the colliculi (mesencephalosynapsis), atresia of the third ventricle (diencephalosynapsis) and corpus callosum abnormalities. In this group, hydrocephalus was present in 100 % of the cases, corpus callosum abnormalities in 66.7 %, pyramidal tract abnormalities in 64.3 % and bilateral or unilateral adducted thumbs in 16.7 %. The retrospective neuropathological diagnosis was: isolated atresia of the aqueduct of Sylvius in 13 cases, isolated mesencephalosynapsis in one case, isolated rhombencephalosynapsis in 2 cases, isolated diencephalosynapsis in 2 cases, mesencephalosynapsis and rhombencephalosynapsis in one case, rhombencephalosynapsis and diencephalosynapsis with no stenosis of the aqueduct of Sylvius in one case, and atresia of the aqueduct of Sylvius combined with encephalocele in one case. In this group, corpus callosum abnormalities consisted of partial agenesis in four cases, total agenesis

Fig. 3 Other uncommonly observed lesions in L1 syndrome: **a** micropolygyria with fusion of the molecular layer (arrow, Case 9) [OM $\times 40$]. **b** Left view of a *LICAM* mutated patient showing pachygyria (Case 57). **c** Ectopic foci of olivary neurons in the dorsal medulla (Case 9) [OM $\times 100$]. **d** Macroscopic view of the tectal hamartoma (arrowhead) (Case 11). **e** Dysplastic, abnormally convoluted dentate nucleus (Case 32) [OM $\times 20$]. *OM* original magnification (scale bar **a**, **c**, **e** 100 μm , **b** 2 cm, **d** 0.5 cm)

in four cases and hypoplasia in two cases. Pyramidal tract abnormalities consisted of hypoplasia in six cases and corticospinal tract asymmetry in one case. Five fetuses had pyramid agenesis in the medulla. One case had five out of the six cardinal signs but instead of aqueductal stenosis, aqueductal atresia-forking was revealed by histology. Thirteen cases were sporadic. In one apparently sporadic case, familial consanguinity was noted. One recurrent case had consanguineous parents. And lastly, an autosomal recessive mode of inheritance was suspected in two families in whom three fetuses were affected.

A polymalformative syndrome was retrospectively diagnosed in seven cases. Two cases, including one with a family history, had VACTERL-H syndrome (MIM#276950). One case had mesencephalosynapsis with cardiac and skeletal abnormalities. In three cases, the syndrome was of unknown aetiology. In one case, autopsy findings suggested a possible Meckel/Joubert syndrome. Among these 7 cases, 85.7 % were males; they presented with hydrocephalus (85.7 %), stenosis of the aqueduct of Sylvius (66.7 %), corpus callosum abnormalities (60 %) and adducted thumbs (50 %). All these cases had less than 5 cardinal signs.

Thirty-five patients had isolated CNS malformations, 85.7 % were male, they presented with a combination of hydrocephalus (71.4 %), agenesis of the corpus callosum (77.4 %), adducted thumbs (15.4 %), stenosis of the aqueduct of Sylvius (45 %) and corticospinal tract abnormalities (47.6 %). Among these, six had a family history of malformation. Only one case (2.9 %) presented with five characteristics, but in fact showed neuropathological signs that were highly suggestive of a tubulinopathy. In three cases belonging to the same family, a bilateral porencephaly was detected suggesting the possible involvement of the *COL4A1* gene. In the last two cases, careful histological review made it possible to determine the cause as post-haemorrhagic hydrocephalus, with the presence of siderophages around the aqueduct of Sylvius in the first case and post-haemorrhagic aqueductal atresia in the second case.

Sixteen fetuses, among which 87.5 % were males, had no mutation in the *LICAM* gene but exhibited phenotypic characteristics similar to *LICAM*-mutated fetuses. These fetuses with “L1-like” syndrome presented with hydrocephalus (100 %), adducted thumbs (61.5 %), corpus callosum agenesis (75 %), stenosis of the aqueduct of Sylvius

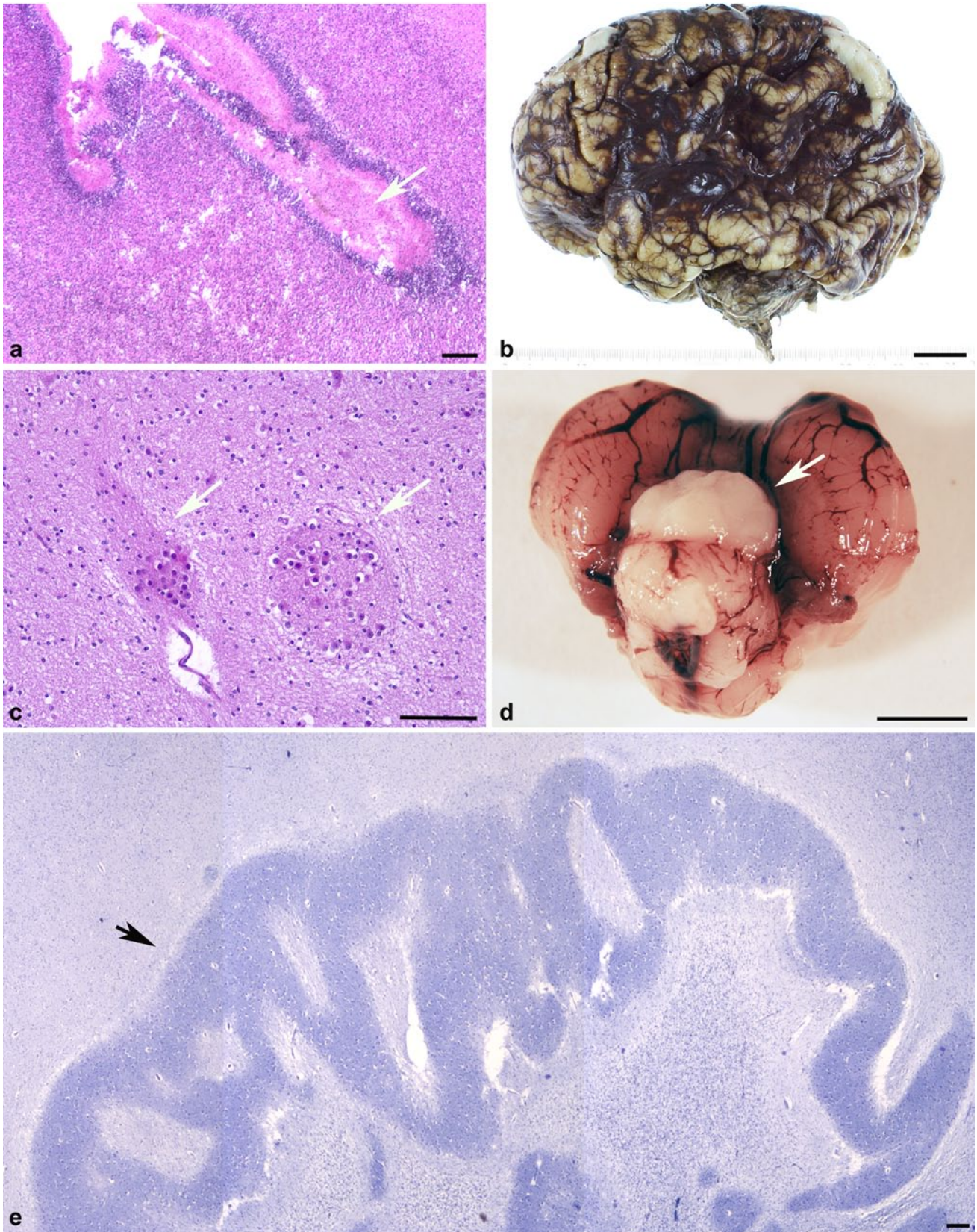


Table 3 Frequency and positive predictive value of the clinical and neuropathological characteristics in the group of patients carrying a mutation compared with the group with no mutation in the *LICAM* gene

Clinical and neuropathological characteristics	Mutation negative			Mutation positive			<i>p</i> value*	Positive predictive value (%)
	Presence of clinical/neuropathological characteristics			Presence of clinical/neuropathological characteristics				
	Yes	No	%	Yes	No	%		
Hydrocephalus	71	8	10	56	0	0	0.021	44
Adducted thumbs	16	43	73	46	6	12	<0.001	74
Corpus callosum abnormalities	49	18	27	43	1	2	<0.001	47
Stenosis of the aqueduct of Sylvius	28	33	54	44	5	10	<0.001	61
Corticospinal tract abnormalities	32	22	41	47	1	2	<0.001	59

* Fisher exact test

(93.7 %) and corticospinal tract abnormalities (87.5 %). In this group, three fetuses were familial cases; ten cases including a female fetus were sporadic cases. One fetus and monozygotic twins from two distinct families had consanguineous parents, but with no recurrence. When considering the overall number of positive criteria per case, assuming characteristics that were not available to be negative, 75 % of fetuses had 5 or 6 characteristics of L1 syndrome. The specificity and sensitivity of these signs are presented in Table 2. From these analyses, it appears that hydrocephalus and corpus callosum anomalies are the most sensitive signs, with sensitivities approaching or reaching 100 %. Whereas hydrocephalus and corpus callosum anomalies have very poor specificities, cortico-spinal tract abnormalities is the only sign combining a very high sensitivity and a fair specificity (98 % sensitivity, 62 % specificity, 2.6 likelihood ratio), making it a potentially useful sign to distinguish between mutated and non mutated fetuses. Conversely, adducted thumbs and stenosis of the aqueduct of Sylvius are the most specific criteria along with cortico-spinal tract abnormalities. This high specificity could be explained by the fact that in milder phenotypes (in living patients), adducted thumbs and/or spastic paraplegia are the key clinical signs of SPG1 or MASA.

Discussion

Genetic screening of the *LICAM* gene and neuropathological hallmarks studied in a series of 138 cases (134 fetuses and 4 newborns) allowed us to identify 5 main groups of patients: (1) fetuses carrying a deleterious mutation in the *LICAM* gene; (2) fetuses with atresia-forking of the aqueduct of Sylvius, sometimes associated with other CNS malformations described in the rhombencephalosynapsis spectrum; (3) fetuses presenting with hydrocephalus due to other malformations restricted to the CNS; (4) hydrocephalus occurring in association with extra-CNS malformations corresponding to known or unknown polymalformative syndromes; and (5) fetuses presenting with a phenotype similar to *LICAM*-mutated fetuses but without any evidence of deleterious mutation in this gene.

We revisited the neuropathological characteristics of the 57 fetuses harbouring a deleterious mutation in the *LICAM* gene, and focused on the six cardinal signs previously described, i.e. sex, hydrocephalus, adducted thumbs, stenosis of the aqueduct of Sylvius, corpus callosum abnormalities and corticospinal tract abnormalities [14, 26, 45].

Hydrocephalus which was present in 100 % of the cases, is considered as the main determinant of the apparent clinical variability in L1 syndrome. As in previous reports, the severity of hydrocephalus in our patients ranged from marginal widening of the lateral ventricles and sometimes of

the third ventricle, to massive ventricular dilatation with macrocephaly, often resulting in pre- or perinatal death [36]. When hydrocephalus has not developed during gestation, children present most of the time with a MASA phenotype. Interestingly, experiments in different animal models also reveal divergent patterns. The first *L1cam* knockout mouse models were generated in two independent laboratories [8, 9]. In the mouse model of Cohen et al. [8], maintained on a 129Sv strain genetic background, ventricular enlargement was not initially reported, but further investigations performed by Fransen et al. [13] using high-resolution magnetic resonance imaging and by Demyanenko et al. [11] using volumetric analysis of histological sections demonstrated slightly dilated ventricles. Dahme et al. [9] showed, in another L1 mutant model backcrossed into the C57Bl/6J and 129 genetic backgrounds, that severe ventricular dilation occurred only in mutants backcrossed into the C57Bl/6J genetic background, suggesting that modifier genes may influence the severity of this L1-related defect. Rolf et al. [33] confirmed these results in the C57Bl/6J model and reported severe hydrocephalus in a new mouse model. The L1-6D knock-in model of Itoh et al. [20] backcrossed into the C57Bl/6 background also showed severe hydrocephalus, supporting the concept of a modifier gene or genes. Nevertheless, it remains unclear how hydrocephaly develops in L1 syndrome, and different hypotheses have been suggested. As reported by Fransen et al. [13], the concomitant loss of neurons that are unable to project through the corpus callosum to contralateral homotypic areas and of neurons which normally give rise to the corticospinal tracts, as well as the increase in brain compliance due to the loss of L1-mediated adhesion between axons might be responsible for white and grey matter atrophy and ventricular dilatation. However, it has been pointed out that neither hypothesis can explain the occurrence of high-pressure hydrocephalus in some human L1 syndromes [13].

Stenosis of the aqueduct of Sylvius was observed in 89.8 % (44/49) of the cases; the five other patients had a normal aqueduct. Even though hydrocephalus was associated with stenosis of the aqueduct of Sylvius in the original description by Bickers and Adams, many patients displaying a patent aqueduct have been reported thereafter [17, 26, 45]. In the L1-deficient mice generated by Cohen et al. [8] and Fransen et al. [13], the aqueduct, although abnormally shaped, was normal in size, whereas two other experimental studies observed a dilated aqueduct or no consistent difference in the morphology of the aqueduct between wild-type mice and L1 mutants [11, 33]. Therefore, stenosis of the aqueduct probably results from the deformation of the brain by massively enlarged ventricles, which in turn provokes the compression of the aqueduct and subsequently, high-pressure hydrocephalus. In the same manner, the fusion or apposition of the thalami observed in seven of

our cases as well as the deformation of the hippocampus may also be related to hydrocephalus. Notably, mouse hippocampi were described as histologically normal or with fewer pyramidal and granule cells [9, 11, 33].

Corpus callosum and corticospinal tract abnormalities were present in 97.7 and 97.9 %, respectively, of the cases with adducted thumbs due to corticospinal tract abnormalities in 88.5 %. Despite the high sensitivity, calculated at 97.73 %, of corpus callosum abnormalities, these were not a very informative criterion (specificity at 26.87 %). This fact could be partly due to the damage to midline structures at the time of autopsy, implying the necessity for careful US or MRI examinations in order to improve the diagnosis of L1 syndrome and the mutation detection rate. In humans, lower limb spasticity has been linked to corticospinal tract hypoplasia or agenesis [15, 22]. From experiments based on the expression pattern of L1 in the developing nervous system and on its complex interactions, it has been shown that L1 plays crucial roles in neuronal migration, patterning and axonal extension, pathfinding, fasciculation, neuronal survival and synaptic plasticity [25, 28, 29, 35, 44, 46]. Direct genetic evidence for the implication of L1 in axonal guidance has only been provided by mouse models harbouring null mutations [8, 9]. Similar to L1 patients, these L1-deficient mice display reduced decussation, a reduced number of corticospinal axons in the dorsal columns of the spinal cord and a reduced size of the corticospinal tracts. Morphometric analyses have also demonstrated that partial agenesis of the corpus callosum with the occurrence of Probst bundles is related to the failure of callosal axons to cross the midline [11].

Cerebellar lesions were frequently observed in our series. Global cerebellar hypoplasia (biometric data <5th percentile) were noted in six cases. Vermis hypoplasia was identified in a single foetus aged 32 weeks, and dysplastic or fragmented dentate nuclei were observed in 6 (22.8 % of the cases). In an MRI study carried out in 96 children aged 5 days to 8 years with L1CAM loss-of-function mutations, 3 had total vermis hypoplasia, and 7 partial anterior vermis hypoplasia (9.6 % of the cases) [21]. The higher rate of cerebellar anomalies in our series may be explained, at least partly, by the fact that our cases represent the most severe form of L1 syndrome, and by in vitro studies showing that L1 is implicated in cerebellar granule cell migration and neurite outgrowth [28, 30]. Some discrepancies have also been observed in mouse models. In the mutant mice analysed by Dahme et al. [9], all cerebellar cell types were present and the cytoarchitecture of the vermis was preserved with few ectopic neurons observed in the molecular layer, whereas in other L1 knockout mice hypoplasia of the cerebellar vermis [11, 13] or severe atrophy was noted [33].

Lastly, multiple associated visceral malformations have never been reported in L1 syndrome. Some minor

abnormalities such as cleft palate have been reported, as observed in a single case in our series. An association with optic atrophy or Hirschsprung disease has also been documented (no cases in our series), and may be explained by the significant reduction in neural crest cell migration at early developmental stages observed in L1-deficient mice [1, 39]. Renal anomalies consisting in duplication or dilatation of the ureters have also been reported, and may be related to the deleterious effects of the *LICAM* mutation, since the L1 protein has been shown to be expressed in the kidneys. Various renal anomalies have been observed in a boy with a mutation in the *LICAM* gene [27] and in L1 deficient mice [10]. It is worth noting that renal agenesis (1 case) and a cardiac malformation (1 case), which have never previously been reported, were observed in our series.

Among these 138 cases we studied, 57 carried a deleterious or likely deleterious mutation. The mutation detection rate, 41 % here, is higher than the mutation detection rate reported by other groups: 20 % by Vos et al. [42] (72 out of 367 patients) and 30 % by Finckh et al. [12] (46 out of 153 patients). Most of the mutations are private mutations, consistent with previous reports [12, 15, 34, 42, 43]. Importantly, Vos et al. noted that when the mother was not a carrier, 7 % of the mutations occurred de novo in the index case or resulted from germline mutations in the mother. Conversely, if the mother of the index case was a carrier, 10 % of the mutations occurred de novo in the mother or resulted from germline mutations in the index case's grandmother. Therefore, about one mutation in five is a recent mutation, explaining why most of these mutations are private [42].

Despite wide allelic heterogeneity and regardless of the nature of the mutation and its position in the protein, the foetal phenotype based on the six neuropathological criteria was homogeneous. Furthermore, it has already been underlined that the same mutation can be responsible for different forms of L1 syndrome, even within a single family, i.e. HSAS and MASA syndrome [16, 37, 41]. Finally, in our cohort, 68.4 % of the mutations were truncating mutations, a percentage that is quite similar to the 75 % obtained by Vos et al. [42] and the 67 % obtained by Finckh et al. [12]. It is thus difficult to establish a genotype–phenotype correlation, notably between the severity of the disease and truncating or missense mutations.

In order to improve the mutation detection rate, we tried to determine which clinical signs were the most predictive of the presence of an *LICAM* mutation (Tables 2, 3). Each of the cardinal signs was associated with high sensitivity (88.46–100 %) but low specificity (10.13–64.70 %; Table 2), except for adducted thumbs, whose specificity is higher (71.93 %). In addition, the positive predictive value of each of the six cardinal signs was determined with regard to the presence or absence of an *LICAM* mutation

(Table 3). Hydrocephalus had the lowest predictive value, whereas adducted thumbs had the highest. Interestingly, Vos et al. [42], although investigating clinical characteristics after birth, also reached the conclusion that adducted thumbs had the best positive predictive value.

Finally, we compared the percentage of cases displaying five or six reported cardinal signs in the five different neuropathological groups (Table 2). Only a few patients with aqueductal atresia spectrum, CNS malformations or polymalformative syndromes displayed five or more cardinal signs (4.8, 2.9, and 0 %, respectively). Even if we consider as negative the signs that were not evaluated, not mentioned in the report, or not reported even if present, and cases in which it was difficult to carry out a neuropathological examination due to the severity of hydrocephalus or post-mortem autolysis, 80.4 % of the cases with X-linked hydrocephalus presented five or six cardinal signs, while the others displayed four or less cardinal signs. Therefore, when hydrocephalus is associated with at least three or more other cardinal signs, screening of the *LICAM* gene is recommended. Furthermore, neuropathological characteristics displayed higher positive predictive values than clinical characteristics [42]. This could explain differences in mutation detection rates in our series and in the Dutch and German series, which were mainly composed of postnatal forms of the L1 syndrome [12, 42].

These overall findings make it possible to easily exclude several other pathological conditions in order to avoid unnecessary molecular screening for the *LICAM* gene. These other conditions presenting with hydrocephalus occur either against a background of CNS malformations different from those observed in L1 syndrome, or of multiple visceral malformations. Nevertheless, two main alternative diagnoses should be considered: foetal alcohol syndrome (FAS), which was an exclusion criterion in our study, and aqueductal atresia spectrum. Patients with FAS share some features of L1 syndrome that could in part be due to the disruption of L1–L1 binding [32], although this finding has been challenged by another study [4]. It has also been reported that alcohol can inhibit L1-mediated axonal growth [4], but the fact that L1-6D mice do not have axonal growth or guidance defects in the 129/Sv background argues against a loss of L1–L1 adhesion in FAS. Moreover, the diagnosis of FAS is first of all based on the characteristic craniofacial dysmorphism and a maternal history of alcoholism, which are lacking in L1 syndrome. Aqueductal atresia spectrum is the main diagnosis worth discussing, and consists of atresia-forking of the aqueduct of Sylvius, associated most of the time with a fusion of the colliculi, rhombencephalosynapsis, diencephalosynapsis and corpus callosum agenesis [31]. Histological examination of the aqueduct of Sylvius should allow pathologists to rule out a diagnosis of L1 syndrome. Interestingly, from

our series of 21 cases with aqueductal atresia, an autosomal mode of inheritance was highly suspected in 3 families on the basis of recurrence and consanguinity, which highlights the existence of familial forms not reported until now. Finally, 16 cases with no mutations in the *L1CAM* gene displayed the same phenotypic characteristics as in X-linked hydrocephalus, with recurrence in 4 of them. In these L1-like families, exome sequencing is underway in order to identify one (or more) gene(s) responsible for autosomal recessive hydrocephalus. This could potentially contribute to elucidating the pathophysiological mechanisms leading to different forms of hydrocephalus.

Acknowledgments This study was performed in the frame of the European Commission's 7th Framework Programme under GA No 278486, "DEVELAGE" and a "Contrat Interface Inserm" to Homa Adle-Biassette. The authors wish to thank the following fetopathologists for their contribution to this work: Patricia Blanchet (Montpellier), Maryse Bonnière (Paris), Bernard Gasser (Mulhouse), Antoinette Gelot (Paris), Didier Menzies (Nancy), Hanitra Randianaivo (La Réunion). They wish also to thank all the geneticists who set up this series.

Conflict of interest The authors declare that they have no conflict of interest.

References

- Anderson RB, Turner KN, Nikonenko AG, Hemperly J, Schachner M, Young HM (2006) The cell adhesion molecule 11 is required for chain migration of neural crest cells in the developing mouse gut. *Gastroenterology* 130(4):1221–1232
- Barbin G, Aigrot MS, Charles P, Foucher A, Grumet M, Schachner M, Zalc B, Lubetzki C (2004) Axonal cell-adhesion molecule L1 in CNS myelination. *Neuron Glia Biol* 1(1):65–72
- Basel-Vanagaite L, Straussberg R, Friez MJ, Inbar D, Korenreich L, Shohat M, Schwartz CE (2006) Expanding the phenotypic spectrum of L1CAM-associated disease. *Clin Genet* 69(5):414–419
- Bearer CF, Swick AR, O'Riordan MA, Cheng G (1999) Ethanol inhibits L1-mediated neurite outgrowth in postnatal rat cerebellar granule cells. *J Biol Chem* 274(19):13264–13270
- Beasley L, Stallcup WB (1987) The nerve growth factor-inducible large external (NILE) glycoprotein and neural cell adhesion molecule (N-CAM) have distinct patterns of expression in the developing rat central nervous system. *J Neurosci* 7(3):708–715
- Bianchine JW, Lewis RC Jr (1974) The MASA syndrome: a new heritable mental retardation syndrome. *Clin Genet* 5(4):298–306
- Bickers DS, Adams RD (1949) Hereditary stenosis of the aqueduct of Sylvius as a cause of congenital hydrocephalus. *Brain* 72(Pt. 2):246–262
- Cohen NR, Taylor JS, Scott LB, Guillery RW, Soriano P, Furley AJ (1998) Errors in corticospinal axon guidance in mice lacking the neural cell adhesion molecule L1. *Curr Biol* 8(1):26–33
- Dahme M, Bartsch U, Martini R, Anliker B, Schachner M, Mantel N (1997) Disruption of the mouse L1 gene leads to malformations of the nervous system. *Nat Genet* 17(3):346–349
- Debiec H, Kutsche M, Schachner M, Ronco P (2002) Abnormal renal phenotype in L1 knockout mice: a novel cause of CAKUT. *Nephrol Dial Transplant* 17(Suppl 9):42–44
- Demyanenko GP, Tsai AY, Maness PF (1999) Abnormalities in neuronal process extension, hippocampal development, and the ventricular system of L1 knockout mice. *J Neurosci* 19(12):4907–4920
- Finckh U, Schroder J, Ressler B, Veske A, Gal A (2000) Spectrum and detection rate of L1CAM mutations in isolated and familial cases with clinically suspected L1-disease. *Am J Med Genet* 92(1):40–46
- Fransen E, D'Hooge R, Van Camp G, Verhoye M, Sijbers J, Reyniers E, Soriano P, Kamiguchi H, Willemsen R, Koekkoek SK, De Zeeuw CI, De Deyn PP, Van der Linden A, Lemmon V, Kooy RF, Willems PJ (1998) L1 knockout mice show dilated ventricles, vermis hypoplasia and impaired exploration patterns. *Hum Mol Genet* 7(6):999–1009
- Fransen E, Lemmon V, Van Camp G, Vits L, Coucke P, Willems PJ (1995) CRASH syndrome: clinical spectrum of corpus callosum hypoplasia, retardation, adducted thumbs, spastic paraparesis and hydrocephalus due to mutations in one single gene, L1. *Eur J Hum Genet* 3(5):273–284
- Fransen E, Van Camp G, Vits L, Willems PJ (1997) L1-associated diseases: clinical geneticists divide, molecular geneticists unite. *Hum Mol Genet* 6(10):1625–1632
- Fryns JP, Spaepen A, Cassiman JJ, van den Berghe H (1991) X linked complicated spastic paraplegia, MASA syndrome, and X linked hydrocephalus owing to congenital stenosis of the aqueduct of Sylvius: variable expression of the same mutation at Xq28. *J Med Genet* 28(6):429–431
- Graf WD, Born DE, Sarnat HB (1998) The pachygyria-polymicrogyria spectrum of cortical dysplasia in X-linked hydrocephalus. *Eur J Pediatr Surg* 8(Suppl 1):10–14
- Guihard-Costa AM, Larroche JC (1990) Differential growth between the fetal brain and its infratentorial part. *Early Hum Dev* 23(1):27–40
- Guihard-Costa AM, Menez F, Delezoide AL (2002) Organ weights in human foetuses after formalin fixation: standards by gestational age and body weight. *Pediatr Dev Pathol* 5(6):559–578
- Itoh K, Cheng L, Kamei Y, Fushiki S, Kamiguchi H, Gutwein P, Stoeck A, Arnold B, Altevogt P, Lemmon V (2004) Brain development in mice lacking L1–L1 homophilic adhesion. *J Cell Biol* 165(1):145–154
- Kanemura Y, Okamoto N, Sakamoto H, Shofuda T, Kamiguchi H, Yamasaki M (2006) Molecular mechanisms and neuroimaging criteria for severe L1 syndrome with X-linked hydrocephalus. *J Neurosurg* 105(5 Suppl):403–412
- Kenwright S, Jouet M, Donnai D (1996) X linked hydrocephalus and MASA syndrome. *J Med Genet* 33(1):59–65
- Kowitz A, Kadmon G, Eckert M, Schirmacher V, Schachner M, Altevogt P (1992) Expression and function of the neural cell adhesion molecule L1 in mouse leukocytes. *Eur J Immunol* 22(5):1199–1205
- Kujat R, Miragall F, Krause D, Dermietzel R, Wrobel KH (1995) Immunolocalization of the neural cell adhesion molecule L1 in non-proliferating epithelial cells of the male urogenital tract. *Histochem Cell Biol* 103(4):311–321
- Lagenaur C, Lemmon V (1987) An L1-like molecule, the 8D9 antigen, is a potent substrate for neurite extension. *Proc Natl Acad Sci USA* 84(21):7753–7757
- Landrieu P, Ninane J, Ferriere G, Lyon G (1979) Aqueductal stenosis in X-linked hydrocephalus: a secondary phenomenon? *Dev Med Child Neurol* 21(5):637–642
- Liebau MC, Gal A, Superti-Furga A, Omran H, Pohl M (2007) L1CAM mutation in a boy with hydrocephalus and duplex kidneys. *Pediatr Nephrol* 22(7):1058–1061
- Lindner J, Rathjen FG, Schachner M (1983) L1 mono- and polyclonal antibodies modify cell migration in early postnatal mouse cerebellum. *Nature* 305(5933):427–430

29. Luthl A, Laurent JP, Figuero A, Muller D, Schachner M (1994) Hippocampal long-term potentiation and neural cell adhesion molecules L1 and NCAM. *Nature* 372(6508):777–779
30. Michelson P, Hartwig C, Schachner M, Gal A, Veske A, Finckh U (2002) Missense mutations in the extracellular domain of the human neural cell adhesion molecule L1 reduce neurite outgrowth of murine cerebellar neurons. *Hum Mutat* 20(6):481–482
31. Pasquier L, Marcotelles P, Loget P, Pelluard F, Carles D, Perez MJ, Bendavid C, de La Rochebrochard C, Ferry M, David V, Odent S, Laquerriere A (2009) Rhombencephalosynapsis and related anomalies: a neuropathological study of 40 fetal cases. *Acta Neuropathol* 117(2):185–200
32. Ramanathan R, Wilkemeyer MF, Mittal B, Perides G, Charness ME (1996) Alcohol inhibits cell–cell adhesion mediated by human L1. *J Cell Biol* 133(2):381–390
33. Rolf B, Kutsche M, Bartsch U (2001) Severe hydrocephalus in L1-deficient mice. *Brain Res* 891(1–2):247–252
34. Saugier-Verber P, Martin C, Le Meur N, Lyonnet S, Munnich A, David A, Henocq A, Heron D, Jonveaux P, Odent S, Manouvrier S, Moncla A, Morichon N, Philip N, Satge D, Tosi M, Frebourg T (1998) Identification of novel L1CAM mutations using fluorescence-assisted mismatch analysis. *Hum Mutat* 12(4):259–266
35. Schmid RS, Maness PF (2008) L1 and NCAM adhesion molecules as signaling coreceptors in neuronal migration and process outgrowth. *Curr Opin Neurobiol* 18(3):245–250
36. Schrandner-Stumpel C, Fryns JP (1998) Congenital hydrocephalus: nosology and guidelines for clinical approach and genetic counselling. *Eur J Pediatr* 157(5):355–362
37. Schrandner-Stumpel C, Legius E, Fryns JP, Cassiman JJ (1990) MASA syndrome: new clinical features and linkage analysis using DNA probes. *J Med Genet* 27(11):688–692
38. Skaper SD (2012) Neuronal growth-promoting and inhibitory cues in neuroprotection and neuroregeneration. *Methods Mol Biol* 846:13–22
39. Takenouchi T, Nakazawa M, Kanemura Y, Shimozato S, Yamasaki M, Takahashi T, Kosaki K (2012) Hydrocephalus with Hirschsprung disease: severe end of X-linked hydrocephalus spectrum. *Am J Med Genet A* 158A(4):812–815
40. Thor G, Probstmeier R, Schachner M (1987) Characterization of the cell adhesion molecules L1, N-CAM and J1 in the mouse intestine. *EMBO J* 6(9):2581–2586
41. Vits L, Chitayat D, Van Camp G, Holden JJ, Franssen E, Willems PJ (1998) Evidence for somatic and germline mosaicism in CRASH syndrome. *Hum Mutat Suppl* 1:S284–S287
42. Vos YJ, de Walle HE, Bos KK, Stegeman JA, Ten Berge AM, Bruining M, van Maarle MC, Elting MW, den Hollander NS, Hamel B, Fortuna AM, Sunde LE, Stolte-Dijkstra I, Schrandner-Stumpel CT, Hofstra RM (2010) Genotype-phenotype correlations in L1 syndrome: a guide for genetic counselling and mutation analysis. *J Med Genet* 47(3):169–175
43. Vos YJ, Hofstra RM (2010) An updated and upgraded L1CAM mutation database. *Hum Mutat* 31(1):E1102–E1109
44. Welzl H, Stork O (2003) Cell adhesion molecules: key players in memory consolidation? *News Physiol Sci* 18:147–150
45. Willems PJ, Brouwer OF, Dijkstra I, Wilmsink J (1987) X-linked hydrocephalus. *Am J Med Genet* 27(4):921–928
46. Williams EJ, Furness J, Walsh FS, Doherty P (1994) Activation of the FGF receptor underlies neurite outgrowth stimulated by L1, N-CAM, and N-cadherin. *Neuron* 13(3):583–594
47. Wong EV, Kenwrick S, Willems P, Lemmon V (1995) Mutations in the cell adhesion molecule L1 cause mental retardation. *Trends Neurosci* 18(4):168–172